NMR AND CALORIMETRY DETERMINATION OF PORE SIZE AND POROSITY

Fiñana A.[+], Ramia M.E.[*] and Martín C.A.[*,#]
[*] Facultad de Matemática, Astronomía y Física and [+] Facultad de Ciencias Exactas Físicas y Naturales - Universidad Nacional de Córdoba - Córdoba, Argentina.
[#] *Corresponding Author: martin@famaf.unc.edu.ar*

This paper was prepared for presentation at the International Symposium of the Society of Core Analysts held in Calgary, Canada, 10-12 September 2007

ABSTRACT
The present work involves a comprehensive experimental determination of porosity and pore size distribution in rocks from oil field formations by Nuclear Magnetic Resonance (NMR) and Differential Thermal Calorimetry (DTC). Both techniques yield complementary results, the DTC measures the amount of heat involved in a phase transition of the sample under study providing bulk information from which the most abundant pore size can be obtained, the NMR allows the determination of the relative pore size distribution very accurately. Both techniques give complementary information to obtain an absolute pore size distribution.

INTRODUCTION
Nuclear Magnetic Resonance (NMR) as well as Differential Thermal Calorimetry (DTC) are widely used as complementary tools in order to obtain a more detailed explanation of the phenomena under study (Azurmendi et al (2002)). Nevertheless, both techniques provide information from different scales of interactions. While the NMR arises from the local interaction of the proton magnetic moments with a magnetic field, composed by a constant external magnetic plus a local field from neighboring magnetic dipoles and paramagnetic impurities, the DTC measures the bulk enthalpy excess of a sample undergoing a phase transition in respect to a reference material undergoing the same thermal evolution without any phase change (Slichter (1990), Halperin et al (1989)).

Petrophysical information, such as porosity, pore size distribution, bound water, and permeability can be obtained from NMR relaxometry (Kleinberg et al (1994)). The physical process involves the rotation of the proton magnetization, from its stationary equilibrium state to a direction perpendicular to the external magnetic field $\mathbf{B}_0$, followed by the return to equilibrium undergoing two well differentiated relaxation processes. Normally the transverse relaxation, characterized by a time T_2, dephases the spin magnetization faster than the longitudinal relaxation, characterized by T_1, process that involves a return to equilibrium by transferring energy from the spins to the surrounding physical system. The fluid in the pores responds to a spin-echo T_2 experiment with three parallel processes such that

$$\frac{1}{T_2} = \frac{1}{T_{2bulk}} + \frac{1}{T_{2surface}} + \frac{1}{T_{2diffusion}} \quad (1)$$

where T_{2bulk} and $T_{2surface}$ take into account the spin-spin interactions in the bulk and with the pore surface respectively, and the last term is due to the diffusion of the water molecule in an inhomogeneous magnetic field. This term can be made negligible in low magnetic field. Also

$$\frac{1}{T_{2surface}} = \rho_2 \left(\frac{S}{V} \right)_{pore} \tag{2}$$

where the coefficient ρ_2 is the T_2 surface relaxivity strength of the surface (Kleinberg et al (1994)). The most convenient way to measure T_2 is by means of the Carr-Purcell-Meiboom-Gill (CPMG) (Slichter (1990)) pulse sequence, which gives the transversal magnetization decay from which the T_2 distribution is obtained taking a discrete non lineal regularized Laplace transform (Niell et al (2006)), namely the signal amplitude $A(t;C_i,T_{2i})$ is fit by

$$A(t;C_i,T_{2i}) = \sum_{i=0}^{n} \left\{ C_i \, exp\left(-\frac{t}{T_{2i}} \right) - \alpha \left| C_{i+1} - C_i \right| \right\} \tag{3}$$

with the condition that $C_{n+1} = 0$, and where the coefficients C_i indicate the weight of the decay, providing a means to measure the pore abundance whose sizes are characterized by T_{2i}, and α is the regularization coefficient.

The DTC is based on the temperature measurement of two samples, one being the sample under study and the other the reference, undergoing a thermal evolution inside a calorimeter as both gain or loss heat at a given rate. The reference sample is chosen such that it does not have any specific heat anomaly in the temperature range of interest. Any physical change involving a heat evolution of the sample will produce a temperature difference with the reference. The registered temperature difference, between the rock and the reference, yields a characteristic peak typical of a liquid to solid phase transition.

Thus, in a heating up process the transition temperature depends of the brine salinity and the pore size (Strange et al (1993)) according

$$T_f(a) = \frac{k}{a} + T_f(\infty) \tag{4}$$

where

$$a = \left(\frac{V}{S} \right)_{pore} \tag{5}$$

is a measure of the pore size, $T_f(\infty)$ is the brine fusion temperature corresponding to an infinite pore size. It is convenient to rewrite (4) in terms of the temperature shift as

$$\Delta T_f = T_f(a) - T_f(\infty) = \frac{k}{a} \tag{6}$$

Measured values of the constant k (Jehng (1995)) obtained for different compounds are in the range 4.1 10^{-8} *Km* to 7.3 10^{-8} *Km*. Also, studies of samples of controlled pore size (Strange et al (1993)) yield a value of k = 5.7 10^{-8} *Km*. It is reasonable to assume an average value of k = 5.7 10^{-8} *Km*.

Combining equations (2) and (6) follows that the relaxivity constant results

$$\rho_2 = \frac{k}{T_2\,\Delta T_f} = \frac{5.710^{-8}\,Km}{T_2\,\Delta T_f} \tag{7}$$

where $T_2 = T_{2surface}$.

MATERIALS AND METHODS

The studied rocks where obtained from oil bearing geological formations from one prospect oil well of the San Jorge Gulf basin in Argentina. Both rocks are sedimentary sand and its analysis shows that are quite similar although their poral distributions are somewhat different. These are constituted by friable mature equigranular quartzite without cement with high porosity and permeability to saturation, table 1.

Table 1. Composition of the used rocks

	Quartz	Feldspar	Moscovite	Ilmenite and magnetite
Rock 1	95%	2%	1%	2%
Rock 2	93%	3%	2%	2%

The samples were bottled in such a way that the holder was suitable to perform both NMR and DTC measurements without sample handling. This procedure ensures to keep hydration content of the sample unchanged for long periods of time. The sample holder is made of zirconium oxide allowing good thermal conductivity and very low dielectric properties to radio frequency.

The calorimeter is a standard differential thermal calorimeter and the NMR apparatus is a pulsed spectrometer with a working frequency in the range of 2 MHz. for protons resonance frequency, and the T_2 measurements were obtained using CPMG pulse sequence with phase alternation.

EXPERIMENTAL RESULTS

The temperature differences in a cooling process, ΔT, between the samples and the reference versus the reference temperature, T, for rocks 1 and 2, are depicted in figures 1 and 2. Also, ΔT, versus the evolution time, t, as the sample cools down, for both rocks are depicted in figures 3 and 4, the area under these transition peaks is proportional to the number of water molecules undergoing the transition. The figures also include the transition temperatures of the fusion peaks associated to transitions taking place in sets of pores with different sizes.

The spin-spin relaxation times distributions, namely the weight of the decay, C_i, versus the corresponding T_{2i}, are depicted in figures 5 and 6, for rocks 1 and 2. The amplitudes C_i are related to a characteristic pore abundance, and the relaxation time T_{2i} to the pore size.

In order to process the NMR and DTC data by means of equation (7), it is better to summarize the results for rocks 1 and 2 respectively, table 2. Where the two peaks in rock 2 at 268.563 K and 268.541 K have been replaced by one at the average temperature of 268.552 K. The values of T_2 corresponding to the peaks were obtained by fitting the curves, of figures 5 and 6, by two lognormal Gaussian distributions.

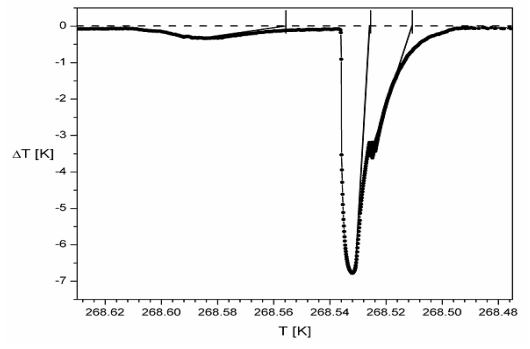

Figure 1: Rock 1, ΔT versus the sample temperature. The standard procedure to obtain the peak temperature extrapolated to the base line is shown in the figure.

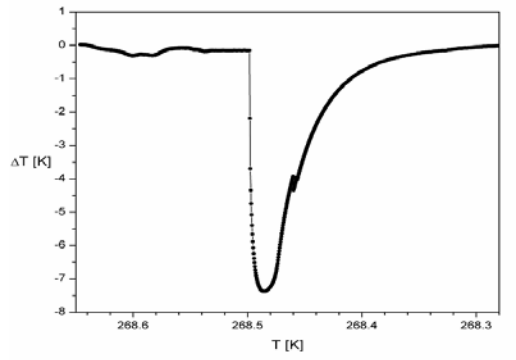

Figure 2: Rock 2, ΔT versus the sample temperature.

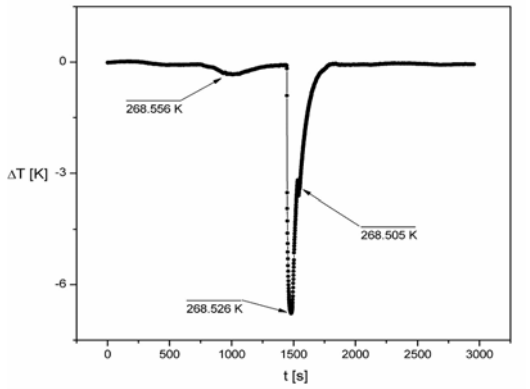

Figure 3: Rock 1, ΔT versus time.

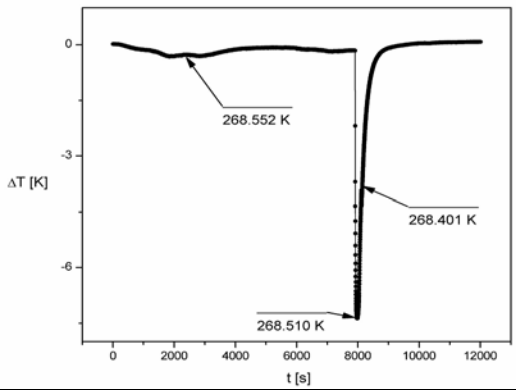

Figure 4: Rock 2, ΔT versus time.

Table 2: Thermodynamic parameters of the used rocks.

	$T_f(\infty)$	$T_f(a)$	$\Delta T_f(a)$	T_2
Rock 1	268.556 K	268.526 K	0.030 K	91.6 10^{-3} s
	268.556 K	268.505 K	0.051 K	20.3 10^{-3} s
Rock 2	268.552 K	268.510 K	0.042 K	94.6 10^{-3} s
	268.552 K	268.401 K	0.151 K	6.5 10^{-3} s

In order to obtain a single valued relaxivity for each rock, we are going to proceed similarly as a T_2 distribution is matched to pore throat size measurements by mercury injection: Namely, the NMR-T_2 distribution is shifted until a "good" correlation is obtained with the mercury injection data. This is achieved by shifting the center of mass of C_i versus T_{2i} distribution to match the center of mass of the percentage porosity occupied by mercury versus pore throat size distribution. Therefore, in this case, the center of mass of temperature shifts is assigned to the center of mass of the C_i versus T_2 distribution. Thus, for rocks 1 and 2 respectively

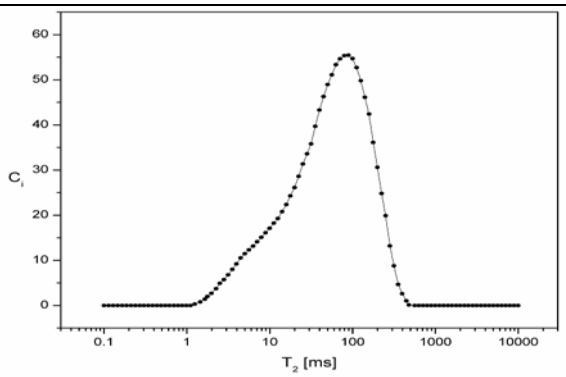

Figure 5: Rock 1, C_i , pore abundance versus T_{2i}.

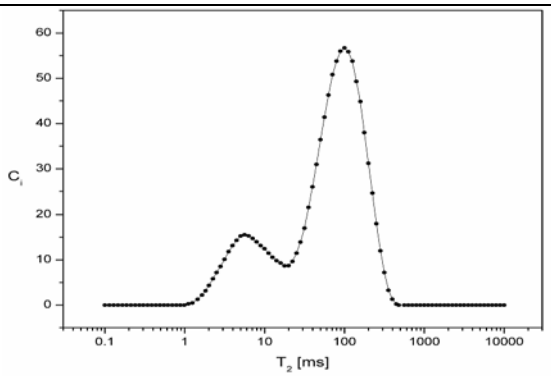

Figure 6: Rock 2, C_i , pore abundance versus T_{2i}.

$T_{2CM}(Rock\ 1)$=76.5 10^{-3} s ; $T_{2CM}(Rock\ 2)$=86.9 10^{-3} s ; $\Delta T_{CM}(Rock\ 1)$=0.035 K ; $\Delta T_{CM}(Rock\ 2)$=0.045 K

The T_{2CM} values are related to the average logarithmic T_2. Therefore, the results yield values of relaxivity given by

$$\rho_2(Rock1) \cong 21\ 10^{-6}\, ms^{-1} \qquad \rho_2(Rock2) \cong 15\ 10^{-6}\, ms^{-1}$$

Considering the errors introduced by the measurements of T_2 and ΔT, the relaxivity values have an error of approximately 8%, being the temperature measurements the dominant figure in the error calculation. It is important to remark that the averaged relaxivity used, for these type of rocks, by loggers is approximately $\rho_2 \cong 15\ 10^{-6}\, ms^{-1}$.

With the relaxivity results the pore size distribution can be plotted in terms of the pore size. Figures 7 and 8 show the pore distribution in addition to the normalized cumulative integral values which allows to extrapolate the average poral size when it reaches a value of 50. In addition, figure 9 shows the absolute cumulative integrals of both rocks, which are related to the rock porosities, and allows to compare the porosities of both rocks.

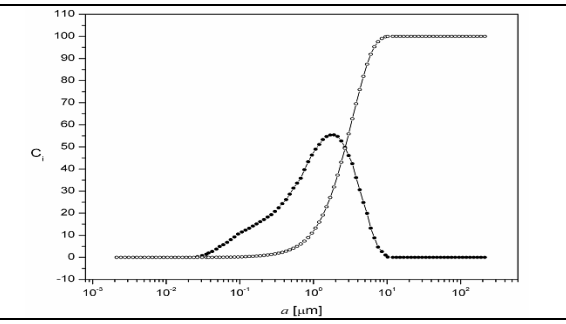

Figure 7: Rock 1, C_i , pore abundance versus a_i, and its normalized cumulative integral.

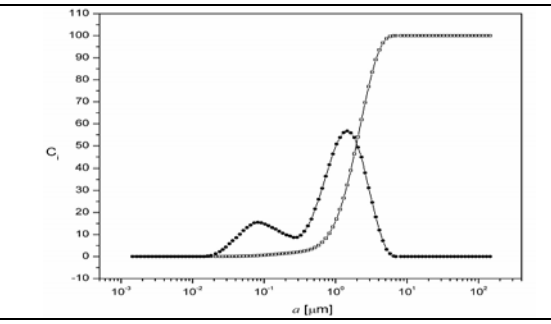

Figure 8: Rock 2, C_i , pore abundance versus a_i, and its normalized cumulative integral.

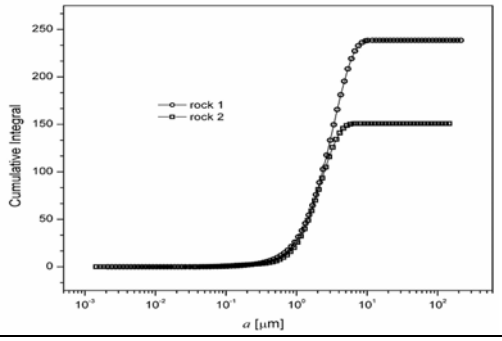

Figure 9: Rocks 1 and 2, cumulative integral versus a_i.

CONCLUSIONS

Measurements of ^{1}H NMR spin-spin relaxation time (T_2) of hydrated samples (plugs) and water fusion temperature by DTC, from which the relaxativity factor was determined. A comparison between the obtained relaxivity factors and the tabulated ones (Coates et al (1999)), i.e.

$$\rho_2(sandstone) \cong 23\ 10^{-6}\, ms^{-1} \quad \rho_2(dolomite) \cong 5.4\ 10^{-6}\, ms^{-1} \quad \rho_2(limestone) \cong 3.2\ 10^{-6}\, ms^{-1}$$

shows that even though both rocks are constituted quite similar, table 1, the relaxivity of rock 1 is closer to a sandstone while the relaxivity of rock 2 takes an intermediate value between a sandstone and dolomite.

The combination of these experimental techniques, NMR and DTC, allows an alternative method when mercury injection data are not available. All of these allow us to conclude that the pores size distributions for both plugs were obtained in a fast and neat non destructive procedure which allows the preservation of the samples for other type of measurements.

ACKNOWLEDGEMENTS

Financial support provided by Universidad Nacional de Córdoba, by the Consejo Nacional de Investigaciones Científicas y Técnicas (through grant PIP 02588), also the company MR Technologies S.A. for the provision of samples. All are gratefully acknowledged.

REFERENCES

Azurmendi H., Ramia M.E., Fiñana A. and Martín C.A., Appl. Mag. Res. **22**, 321 (2002).
Coates R.G., Xiao L. and Prammer M.G., *NMR Logging, Principles and Applications*, Halliburton Energy Services, Houston (1999).
Halpering W.P., D'Orazio F. and Tarczon T.C., *Molecular Dynamics in Restricted Geometries*, John Wiley & Sons, New York (1989).
Jehng J.Y., PhD Thesis, Northwestern University, USA (1995).
Kleinberg R.L., Kenyon W.E. and Mitra P.P., J. Mag. Reson. A **108**, **2**, 206 (1994).
Niell A., Martín C.A. and Ramia M.E., J. Comp. Phys., submitted for publication (2006).
Slichter C.P., *Principles of Magnetic Resonance*, Springer Verlag (1990).
Strange J.H., Rahman M. and Smith E.G., Phys. Rev. Lett. **71**, 3589 (1993).